Research Article

Curcumin Prevents Diabetic Osteoporosis through Promoting Osteogenesis and Angiogenesis Coupling via NF-*κ*B Signaling

Desheng Fan,[1] Jiuqing Lu,[2] Nijia Yu,[2] Yajia Xie [ID],[2] and Lei Zhen [ID][3]

[1]*Department of Pathology, Baoshan Branch, Shuguang Hospital, Shanghai University of Traditional Chinese Medicine, Shanghai 201999, China*
[2]*Oral Biomedical Engineering Laboratory, Shanghai Stomatological Hospital, Fudan University, Shanghai 200001, China*
[3]*Department of Stomatology, Tongji Hospital, School of Medicine, Tongji University, Shanghai 200065, China*

Correspondence should be addressed to Yajia Xie; xieyajia0142@163.com and Lei Zhen; zhenleilei123@126.com

Diabetic osteoporosis (DOP) is a metabolic disease which is characterized by impaired bone microarchitecture and reduced bone mineral density resulting from hyperglycemia. Curcumin, an effective component extracted from *Curcuma longa*, exhibits antioxidation, regulation of bone metabolism and hypoglycemic effects. The BMSC-mediated osteogenesis and angiogenesis coupling seems to be important in bone formation and regeneration. We aimed to explore the effect of curcumin on BMSC-mediated osteogenesis-angiogenesis coupling in high glucose conditions and underlying mechanisms. Our results showed that high glucose impaired the osteogenic and proangiogenic ability of BMSCs and that curcumin pretreatment rescued the BMSC dysfunction induced by high-concentration glucose. Inhibition of the high glucose-activated NF-*κ*B signaling pathway has been found to contribute to the protective effects of curcumin on high glucose-inhibited coupling of osteogenesis and angiogenesis in BMSCs. Furthermore, accelerated bone loss and decreased type H vessels were observed in diabetic osteoporosis mice models. However, curcumin treatment prevented bone loss and promoted vessel formation in diabetic osteoporosis mice. Based on these results, we concluded that curcumin ameliorated diabetic osteoporosis by recovering the osteogenesis and angiogenesis coupling of BMSCs in hyperglycemia, partly through inhibiting the high glucose-activated NF-*κ*B signaling pathway.

1. Introduction

Diabetic osteoporosis (DOP) is becoming an increasing complication of diabetes, which is characterized by destructive bone microarchitecture and reduced bone mineral density (BMD) [1–5]. Compared with normoglycemic individuals, patients with DOP have a significantly increased risk of fractures, leading to high disability and mortality rates [6, 7]. However, an ideal treatment for DOP is currently lacking.

Bone regeneration and remodeling are associated with the osteogenesis and angiogenesis coupling [8, 9]. Meanwhile, cross-talk between BMSCs and endothelial cells seems to be vital in bone regeneration [10–13]. Endothelial cells are largely dedicated to the improvement of the recruitment and osteogenic differentiation of BMSCs. Conversely, BMSCs

secrete multiple proangiogenic growth factors to promote angiogenesis and tissue regeneration. However, much evidence has shown that the declined osteogenic differentiation function and angiogenesis ability of BMSCs is an important mechanism of DOP [14–17]. Therefore, restoring the damaged osteogenesis and angiogenesis function of BMSCs is crucial for the treatment of DOP.

Curcumin, an effective component extracted from *Curcuma longa,* exhibits antioxidation, regulation of bone metabolism, and hypoglycemic effects [18–26]. Reports demonstrate that curcumin may ameliorate bone microarchitecture and enhance BMD in APP/PS1 transgenic mice [27] and has shown bone protective effect on postmenopausal osteoporosis animal models and patients [28–32]. More importantly, recent studies have found the therapeutic value of curcumin on osteoporosis induced by

diabetes [33, 34]. The benefits of curcumin on bone formation and regeneration are attributed to its capacity to reduce H_2O_2-stimulated osteoblast apoptosis [35], improving osteoblast mitochondrial function [36], and recovering the high glucose-impaired osteogenic differentiation of osteoblast and BMSCs [37, 38]. However, the effect of curcumin on BMSCs-mediated osteogenesis and angiogenesis coupling in high glucose microenvironments and the mechanisms underlying it are not clear.

NF-κB, which is known as a master transcription factor, contributes to the development of diabetes and its complications. Inactivation of NF-κB can reduce inflammatory cytokine secretion in diabetic animal models and patients [39, 40]. Furthermore, studies have discovered that NF-κB signaling pathway have a significant influence on osteoporosis therapy and bone regeneration [41, 42]. Downregulation of NF-κB p65 expression drastically alleviates osteoporosis in OVX mice [43]. The activated NF-κB signaling pathway inhibits BMSCs mediation of the bone regeneration and angiogenesis in a distraction osteogenesis model [44]. Hence, these findings demonstrate that inhibiting overactivated NF-κB pathway may be a new way for the treatment of diabetes and osteoporosis.

We aimed to investigate whether curcumin could rescue high glucose-inhibited osteogenesis and angiogenesis of BMSCs. In addition, we examined whether inhibiting overactivated NF-κB signaling pathway contribute to the protective effects of curcumin on BMSCs dysfunction. Furthermore, we used a DOP model to explore the effects of curcumin on bone regeneration and vessel formation *in vivo*. The current study laid the foundation for curcumin in the treatment of DOP.

2. Materials and Methods

All animal protocols and experiments were approved by the Institutional Committee for Animal Use and Care at Shanghai University of Traditional Chinese Medicine.

2.1. Cell Cultures.
C57BL/6 male mice of six-week-old (SLAC Laboratory Animal Co. Ltd., China) were used to obtain bone marrow samples. BMSCs were isolated from the bone marrow. The cells were inoculated in culture dishes containing DMEM (HyClone) and 10% FBS (Gibco). BMSCs from passages 2–4 were used in our study.

2.2. Cell Viability.
BMSCs were treated with curcumin (Cur; Sigma-Aldrich) from $0.1\,\mu$M to $10\,\mu$M for 48 hours. After that, a CCK-8 kit was used to measure the cell viability.

2.3. BMSCs Osteogenic Differentiation.
Cells were cultured with 5.5 mM glucose as the control group (NG), and BMSCs treated with 33 mM glucose represented the high glucose group (HG). For the curcumin groups, cells were cultured with 33 mM glucose and $1\,\mu$M curcumin (HG + Cur). After seven days of osteogenic induction, ALP staining analysis and ALP activity was detected. After 21 days of culture,

calcium nodules were detected through staining with a 2% alizarin red S solution (Solarbio, China).

2.4. Quantitative Real-Time PCR (qRT-PCR) Analysis.
Total RNA was extracted using TRIzol reagent (Tiangen, China). One microgram of cDNA templates was used for qRT-PCR analysis. The expression of the mRNAs was calculated via the comparative cycle threshold method against GAPDH. The primers were as follows:

Runx2 F: 5′CTCAGCAGCAGCAGCAGCAG3′, R: 5′GCACGGAGCACAGGAAGTTGG3′; OCN F: 5′GAATCGGGGGGATGTACCCAC3′, R: 5′CGAAGGCCTCTGGTTCCACT3′; OSX F: 5′GGATTGGATCTGAGTGAGCC3′, R: 5′GCCATAGTGAGCTTCTTCCTGG3′; VEGF F: 5′CGAGCAGCGAAAGCGACAGG3′, R: 5′CGAAGCGAGAACAGCCCAGAAG3′; GAPDH F: 5′GTCCATGCCATCACTGCCACTC3′, R: 5′CGCCTGCTTCACCACCTTCTT3′.

2.5. Conditioned Medium (CM) of BMSCs.
After 48 hours of treatment with or without curcumin, BMSCs were cultured in fresh DMEM for an additional 48 hours. Then, the CM from each group (CM^{NG} group, CM^{HG} group, and CM$^{HG + Cur}$ group) was harvested.

2.6. Enzyme-Linked Immunosorbent Assay (ELISA).
An ELISA kit (Beyotime Biotechnology, China) was used to detect the concentration of VEGF in different conditioned media.

2.7. EdU Analysis.
HUVECs were cultured with different CM for 24 hours and incubated in EdU working solution (Beyotime Biotechnology, China) for 2 hours. After fixation for 15 minutes with 4% paraformaldehyde, cells were treated with the click additive solution for another 15 min. Finally, the nuclei were stained using a Hoechst solution.

2.8. Scratch Wound Assay.
HUVECs were inoculated in six-well plates and grown to 100% confluence. Two parallel scratches were generated in each well using a $200\,\mu$L pipette tip, and the medium was replaced with CM. After 24 hours, the scratched areas were measured.

2.9. Tube Formation.
Cells were inoculated onto Matrigel-coated 96-well plates and cultured with different CM for 24 hours. The tubule number and lengths were quantified using ImageJ software.

2.10. Immunofluorescence Staining.
BMSCs were incubated with an anti-p65 antibody (1 : 200; Abcam, United Kingdom) at 4°C overnight and were treated with secondary antibody (1 : 500; Cell Signaling Technology) in the dark for another 1 hour.

2.11. Western Blot.
Cells were lysed with RIPA lysis buffer for 30 min and proteins were extracted. Protein samples were electrophoresed on 5–12% SDS-polyacrylamide gels.

The pretreated PVDF membrane (Invitrogen) was used to transfer the fractionated proteins. Then, the PVDF membrane was blocked for 1 hour and incubated with anti-p65 (1 : 1,000; Abcam), anti-phosphorylated p65 (p-p65; 1 : 500, Abcam), anti-Runx2 (1 : 1,000; Cell Signaling Technology), anti-VEGF (1 : 1,000; Cell Signaling Technology), anti-β-actin (1 : 2000; Cell Signaling Technology), anti-GAPDH (1 : 2,000; Cell Signaling Technology), and anti-LaminB (1 : 2,000; Cell Signaling Technology) primary antibodies overnight at 4°C. The membrane was incubated in the secondary antibodies (1 : 5,000; Invitrogen) for 1 hour.

2.12. Animals and Treatment. Fifteen six-week-old C57BL/6 male mice received intraperitoneal injections of streptozotocin (STZ, 50 mg/kg; Sigma-Aldrich) to induce DM. At three and seven days after STZ injection, the fasting blood glucose (FBG) was detected using a glucometer (OMRON, Japan). Only mice with FBG two times higher than 16.7 mmol/L were considered successful models of DM [45–48]. Twelve mice fit the criterion and were divided into two groups ($n = 6$ mice per group) according to the treatment: DM and DM + curcumin (DM + Cur). The other six mice were grouped into the control group. Curcumin was administered via gavage at a dose of 100 mg/kg/day for eight weeks after the establishment of the DM model.

2.13. Micro-CT Analysis. At the end of these experiments, the mouse femur samples were analyzed using a micro-CT system. The region of interest (ROI) was selected and the following parameters were calculated.

2.14. Microfil Perfusion. Cardiac Microfil (FlowTech) perfusion was performed to evaluate the neovascularization. Subsequently, the perfused mice were placed at 4°C for 24 h, and then the femur samples were decalcified for four weeks. The vessel formation were analyzed using a micro-CT system.

2.15. Immunofluorescence Staining of Bone Tissue. The sections were incubated with a CD31 antibody (1 : 100; Abcam) and an endomucin (EMCN) antibody (1 : 100; Santa Cruz) together at 4°C overnight and then were incubated with secondary antibodies (1 : 200; Santa Cruz) for 1 hour. The images were photographed with a camera. The CD31hiEmcnhi type vessels were measured using Image-Pro Plus software based on color recognition.

2.16. Statistical Analysis. All experimental data are presented as mean ± SD and the statistical analysis was tested using Student's *t*-test and one-way ANOVA with SPSS 17.0 software.

3. Results

3.1. Curcumin Rescued the High Glucose-Inhibited BMSCs Osteogenic Differentiation. CCK-8 results showed that curcumin ranging from 0.1 μM to 1 μM was not significantly influenced on cell viability; however, 5 μM and 10 μM curcumin decreased cell viability (Figure 1(a)). Several studies have suggested that high concentrations of glucose can suppress the BMSCs osteogenic differentiation. We, therefore, determined whether curcumin could rescue the high glucose-induced osteogenic dysfunction of BMSCs *in vitro*. Our results demonstrated that curcumin pretreatment significantly reversed the decrease in ALP staining and activity induced by high glucose (Figure 1(b)). Similarly, alizarin red staining and semiquantitative analysis results also showed that the reduced mineralization nodule formation under high glucose conditions was recovered by curcumin (Figure 1(c)). Furthermore, the decreased mRNA and protein expression of osteogenic markers in high glucose conditions was recovered by curcumin administration (Figures 1(d)–1(f)). These findings revealed that curcumin promoted BMSCs osteogenic differentiation in high glucose.

3.2. Curcumin Recovered the High Glucose-Impaired Proangiogenic Ability of BMSCs. Based on the results of the EdU test, HUVECs cultured in CM^{HG} showed decreased proliferation compared with cells cultured with CM^{NG}; however, CM$^{HG + Cur}$ treatment significantly reversed the decrease in proliferation induced by CM^{HG} (Figures 2(a) and 2(b)). In addition, the migration capacity of HUVECs was suppressed after stimulation with CM^{HG}, and the migration area was significantly increased in the CM$^{HG + Cur}$ group compared with the CM^{HG} group (Figures 2(c) and 2(d)). Moreover, CM^{HG} markedly impaired the tube formation ability of HUVECs compared to that of the CM^{NG} group; however, CM$^{HG + Cur}$ treatment significantly rescued the tube formation of HUVECs cultured with CM^{HG} (Figures 2(e)–2(g)).

3.3. Curcumin Promoted the Angiogenesis Potential of BMSCs by Increasing VEGF Expression and Secretion. In the present study, we observed markedly reduced VEGF protein expression in BMSCs exposed to HG compared with cells exposed to NG, whereas the HG-induced suppression of VEGF expression was reversed by curcumin (Figures 3(a) and 3(b)). Moreover, the production of VEGF in the CM from high glucose-induced BMSCs was much lower than that in the normal glucose group and that curcumin pretreatment increased the concentration of VEGF from high glucose + curcumin group (Figure 3(c)). To further investigate whether VEGF mediated curcumin-promoted angiogenesis in high glucose conditions, VEGF neutralizing antibodies were used. As shown in Figures 3(d)–3(j), blocking VEGF remarkably suppressed the curcumin-enhanced angiogenesis capacity of BMSCs in high glucose.

3.4. NF-κB Signaling is Involved in the Effects of Curcumin on BMSCs-MediatedOsteogenesis-Angiogenesis Coupling. Western blot results showed that high-concentration glucose increased the phosphorylation levels of NF-κB p65 (p-p65) without changing the total NF-κB p65 levels (Figures 4(a) and 4(b)). However, curcumin decreased p-p65 levels promoted by high glucose (Figure 4(c)). In
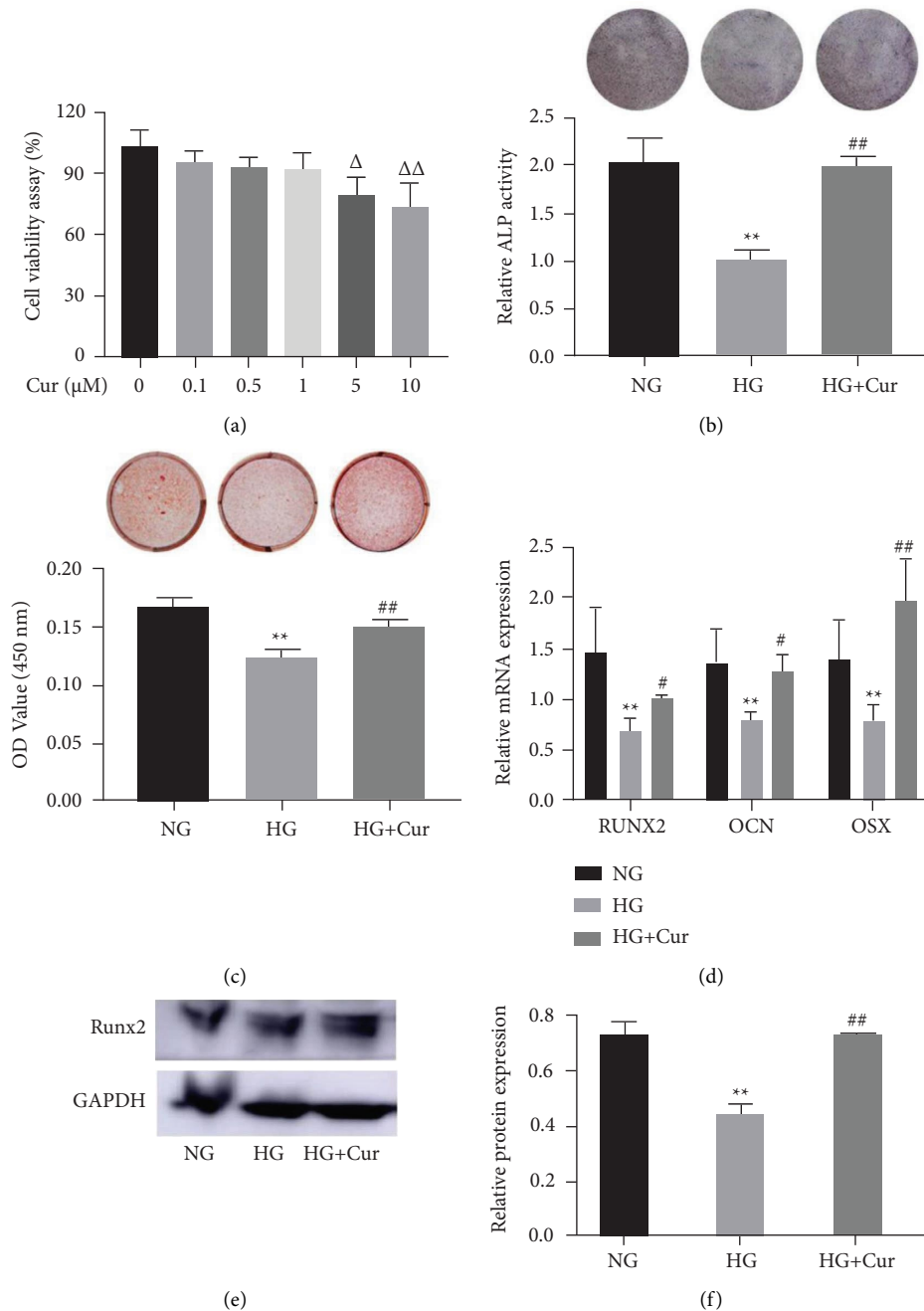
(a)

(b)

(c)

(d)

(e)

(f)

FIGURE 1: Curcumin (Cur) rescued HG-induced osteogenic dysfunction of BMSCs. (a) Cell viability was determined by CCK-8 in the presence of different concentration of Cur for 24 h. (b)–(f) Osteogenic differentiation of BMSCs treated with Cur and different concentrations of glucose were determined with (b) ALP staining and ALP activity assays; (c) alizarin red staining and calcium deposition analysis; (d) expression of osteogenic-specific genes were assessed with qRT-PCR; (e)–(f) the expression of Runx2 by western blot. Data are presented as the mean ± SD from at least three independent experiments. $^{\Delta}p < 0.05$, $^{\Delta\Delta}p < 0.01$, versus 0μM Cur group. $^{*}p < 0.05$ and $^{**}p < 0.01$ versus NG group. $^{#}p < 0.05$ and $^{##}p < 0.01$ versus HG group.

addition, high glucose upregulated the nuclear protein expression of NF-κB p65 in BMSCs, whereas curcumin treatment attenuated nuclear NF-κB p65 (Figure 4(d)). Immunofluorescence assays also found that the nuclear localization of the NF-κB p65 protein in curcumin-treated cells was weaker than that in high glucose-stimulated cells (Figures 4(e) and 4(f)).

We subsequently explored whether the coupling of osteogenesis-angiogenesis in high glucose could be impacted by modulating NF-κB signaling. Our results showed that cells cultured in high glucose supplemented with Bay117082, a specific NF-κB inhibitor, exhibited decreased p-p65 activity compared with that of cells incubated with high glucose only (Figures 5(a) and 5(b)). However, ALP and
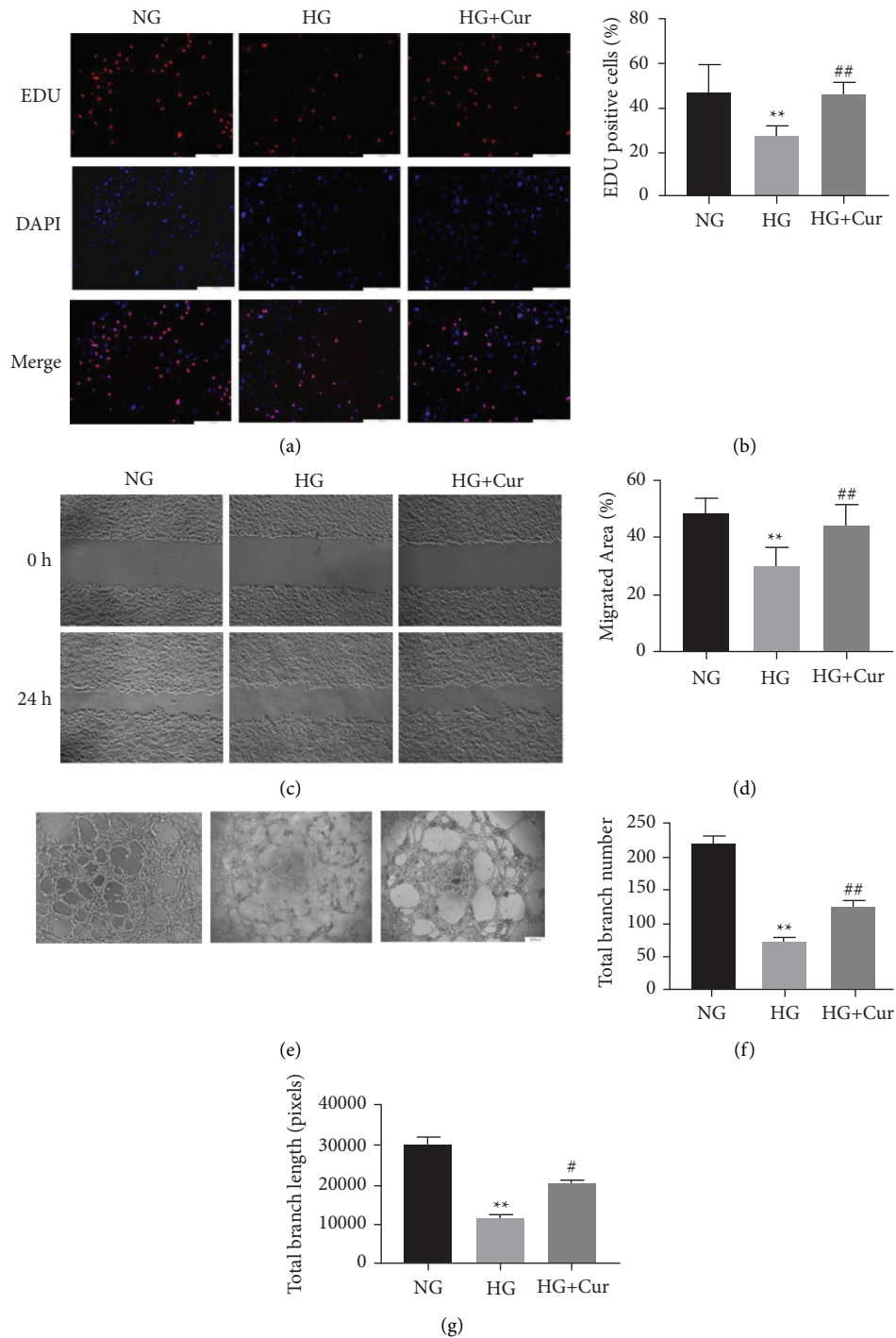
(a)

(b)

(c)

(d)

(e)

(f)

(g)

FIGURE 2: Cur recovered HG-impaired proangiogenic ability of BMSCs. Endothelial cells stimulated with conditioned medium (CM) from BMSCs treated with NG, HG, and HG + Cur. (a)–(b) Proliferation was determined by EDU555 staining. (c)–(d) Endothelial cell motility in each group was evaluated using the scratch wound assay. (e)–(g) Representative images (e) and quantification of tube formation (f)–(g) were assessed in each group. Data are presented as the mean ± SD from at least three independent experiments. $^*p < 0.05$ and $^{**}p < 0.01$ versus NG group. $^#p < 0.05$ and $^{##}p < 0.01$ versus HG group.

alizarin red staining results showed that BMSCs treated with Bay117082 exhibited substantially higher levels of ALP activity and mineralization nodule formation than cells treated with high glucose (Figures 5(c) and 5(d)). Moreover, the suppressed migration and tube formation ability of

HUVECs stimulated with CM^{HG} was reversed by treatment with CM$^{HG + Bay117082}$ (Figures 5(e)–5(h)). We also observed that Bay117082 significantly upregulated osteogenesis and angiogenesis-related proteins Runx2 and VEGF expression (Figures 5(i) and 5(j)). All these data suggested that

(a)

(b)

(c)

(d)
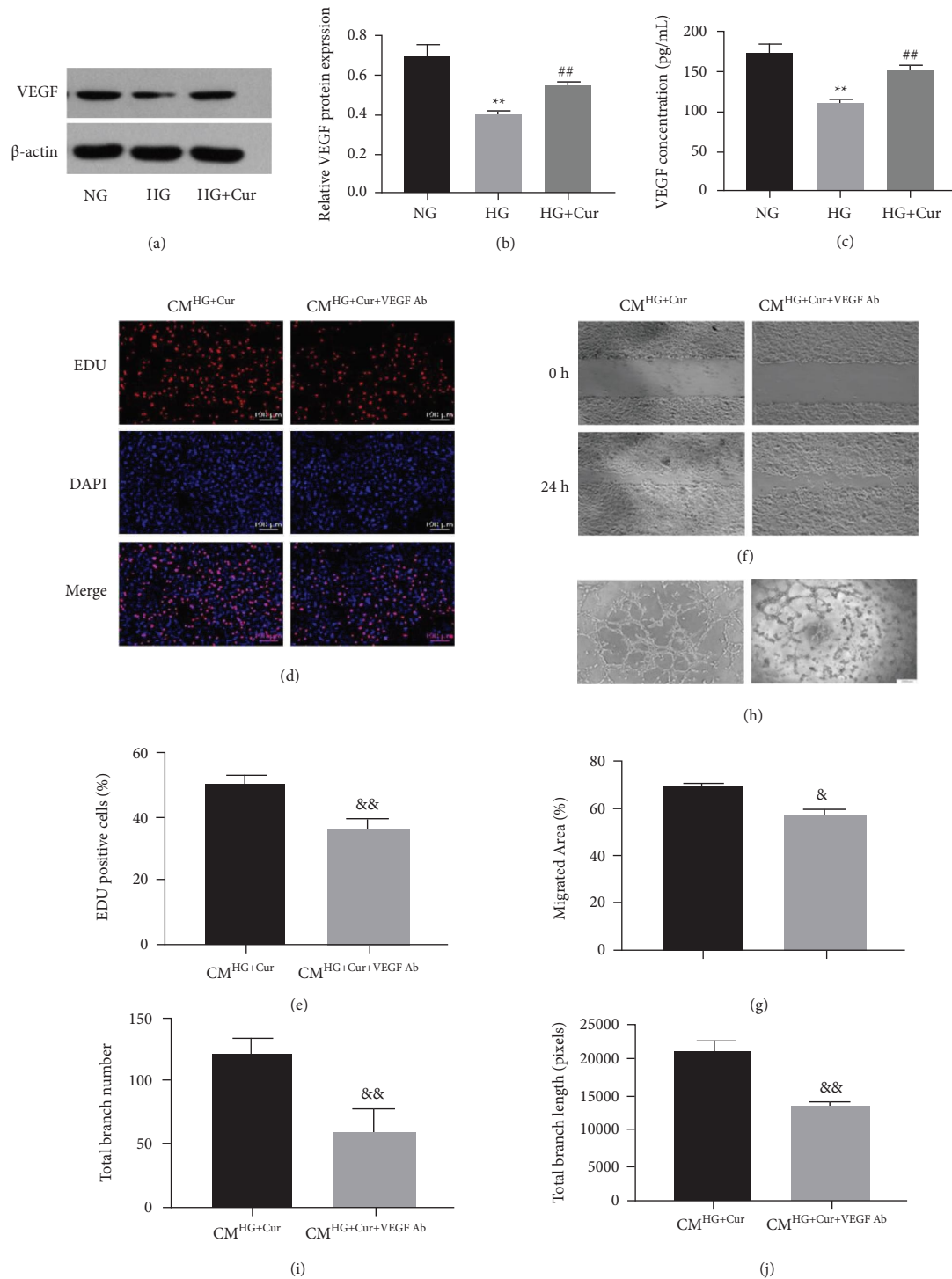
(f)

(h)

(e)

(g)

(i)

(j)

FIGURE 3: Cur increased VEGF expression and secretion to improve the proangiogenic capacity of BMSCs in HG. (a)–(b) VEGF protein expression of BMSCs in each group were assessed using western blot. (c) Detection of VEGF concentration in conditioned medium from BMSCs in each group using ELISA. (d)–(j) Endothelial cells were incubated with Cur pretreated BMSC CM, supplemented with or without VEGF neutralizing antibodies. (d)–(e) Proliferation was determined by EDU555 staining. (f)–(g) Cell motility in each group was evaluated using the scratch wound assay. (h)–(j) Representative images and quantification of tube formation were assessed in each group. Data are presented as the mean ± SD from at least three independent experiments. $^{*}p < 0.05$ and $^{**}p < 0.01$ versus NG group. $^{\#}p < 0.05$ and $^{\#\#}p < 0.01$ versus HG group. $^{\&}p < 0.05$ and $^{\&\&}p < 0.01$ versus CMHG + Cur group.
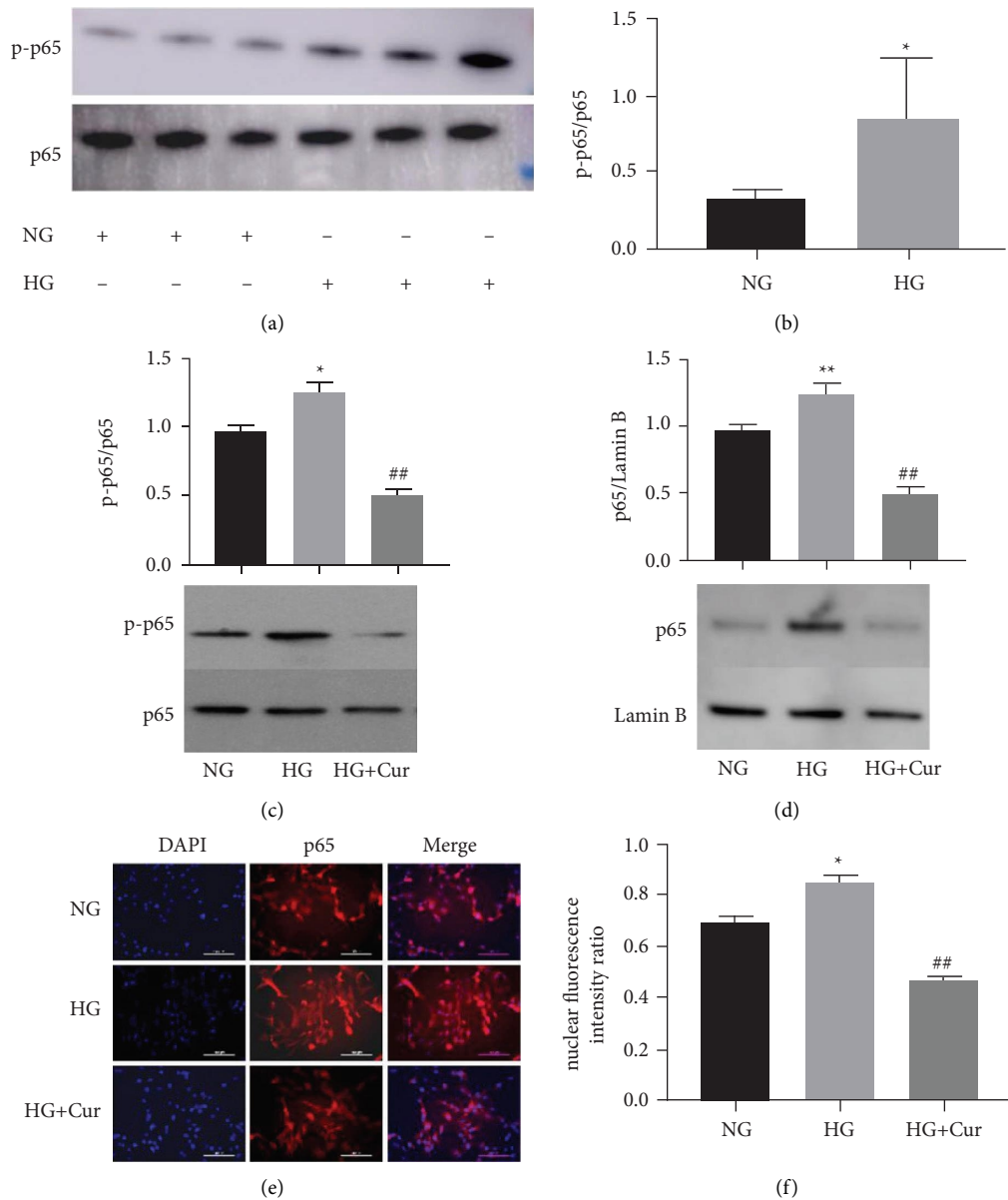
(a)

(b)

(c)

(d)

(e)

(f)

FIGURE 4: Cur regulated NF-κB signaling in BMSCs. (a)–(b) Western blot of p65 and p-p65 in BMSCs treated with NG and HG. (c) Western blot of p65 and p-p65 in BMSCs treated with NG, HG, and HG + Cur. (d) The nuclear protein levels of p65 were detected by western blot in NG, HG, and HG + Cur group. (e) BMSCs were fixed and incubated with an anti-p65 antibody. Nuclei were stained by DAPI. The nuclear and cytoplasm images were merged in the same visual field. (f) Quantitative analysis of the nuclear translocation of p65. Data are presented as the mean ± SD from at least three independent experiments. $^{*}p < 0.05$ and $^{**}p < 0.01$ versus NG group. $^{#}p < 0.05$ and $^{##}p < 0.01$ versus HG group.

curcumin action on BMSCs-mediated osteogenesis-angiogenesis couples partly through the NF-κB signaling pathway.

3.5. Curcumin Prevented Diabetes-Induced Bone Loss and Promoted Vessel Formation.
The micro-CT results showed that curcumin treatment rescued the reductions of BV/TV, Tb. N, Tb. Th, and BMD in DM mice (Figures 6(b)–6(g)).

The microfil showed a reduced vessel network in the DM group while more vessel formation was detected in the DM + curcumin group (Figure 6(h)). Furthermore, the role of curcumin in type H vessel was investigated. Immunofluorescence staining showed that curcumin administration increased the number of type H vessels in DM mice (Figures 6(i) and 6(j)). These results revealed that curcumin treatment prevented diabetes-induced bone loss and promoted vessel formation *in vivo*.
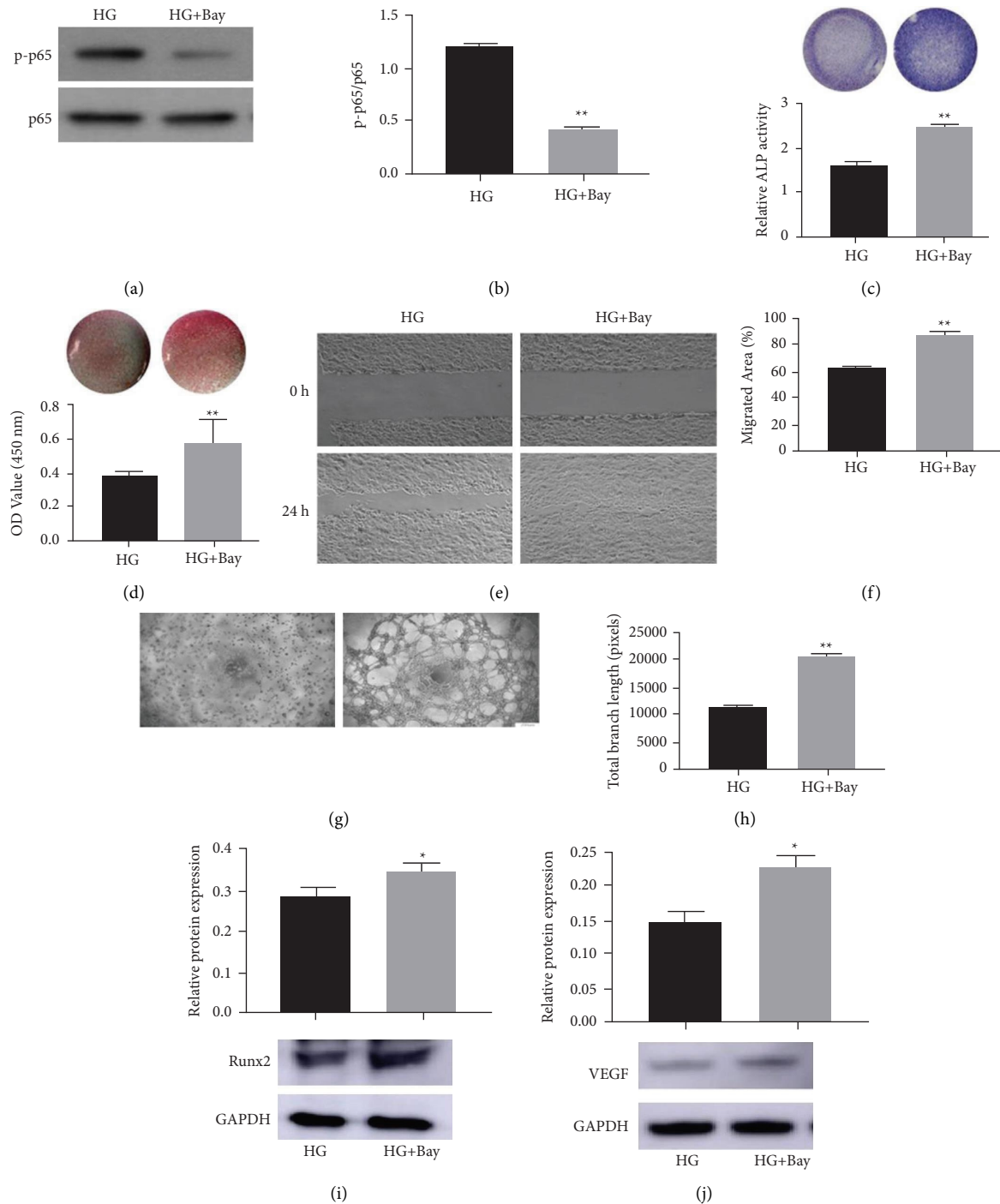
FIGURE 5: NF-κB signaling is involved in HG-inhibited osteogenic differentiation and proangiogenic ability of BMSCs. Western blot of p65 and p-p65 in BMSCs treated with HG or HG + Bay117082 (Bay) (a) and (b). Osteogenic differentiation of BMSCs treated with HG or HG + Bay were determined with (c) ALP staining and ALP activity assays, and (d) alizarin red staining and calcium deposition analysis. Endothelial cells stimulated with conditioned medium from BMSCs treated with HG or HG + Bay. (e) and (f) Endothelial cell motility in each group was evaluated using the scratch wound assay. (g) and (h) Representative images and quantification of tube formation were assessed in each group. (i) and (j) Expression of Runx2 and VEGF protein in each group by western blot. Data are presented as the mean ± SD from at least three independent experiments. $^{*}p < 0.05$ and $^{**}p < 0.01$ versus HG group.

(a)

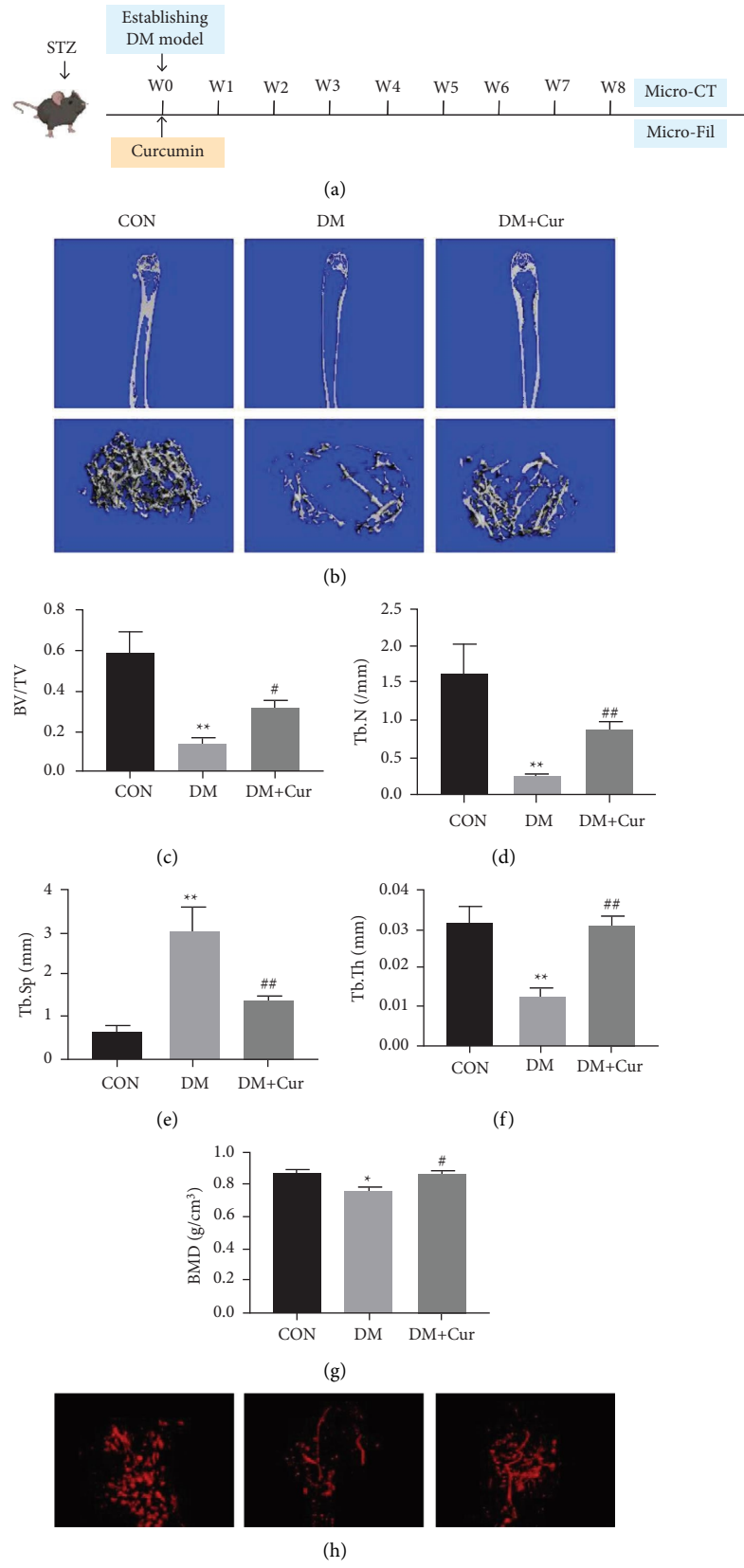(b)

(c)

(d)

(e)

(f)
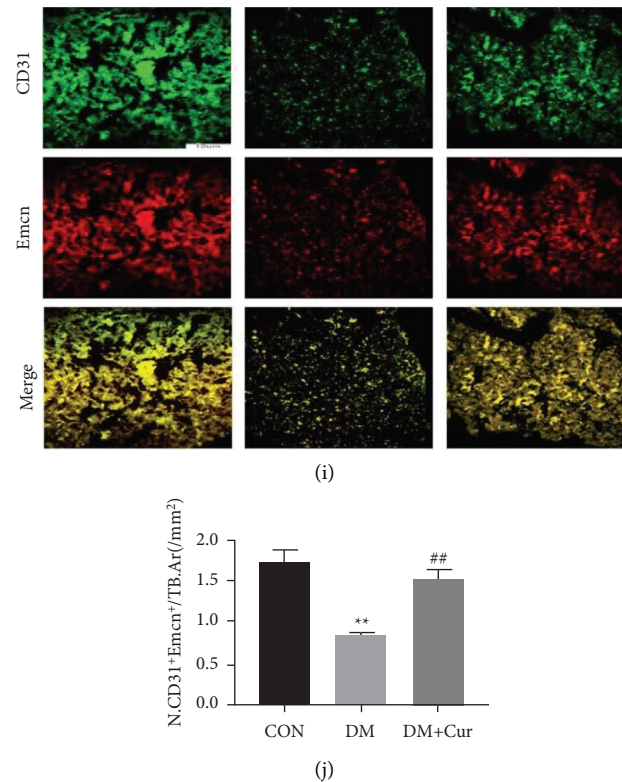

(g)

(h)

Figure 6: Continued.

(i)

(j)

FIGURE 6: Cur prevented diabetes-induced bone loss and promoted vessel formation *in vivo*. (a) Experimental design illustrating the time points for inducing diabetes by STZ, establishing the DM model, and the timing of curcumin administration in the animal model. (b)–(g) Micro-CT images and (b) quantitative CT analysis (c)–(g) were performed in the distal femur from normal mice, DM mice, and DM mice treated with Cur. (h) Images of microfil perfusion. (i) Representative immunostaining images for CD31 (green) and EMCN (red) in the distal femur. (j) The Emcn^{hi} CD31^{hi} (yellow) cells were quantified. Data are shown as mean ± SD. $^{*}p < 0.05$ and $^{**}p < 0.01$ versus CON group. $^{#}p < 0.05$ and $^{##}p < 0.01$ versus DOP group.

4. Discussion

Some studies have proven that osteogenesis and angiogenesis coupling plays a vital role in the pathogenic progression of DOP [14–17]. In the study, we demonstrated that curcumin treatment could enhance BMSC-mediated osteogenesis and angiogenesis coupling in high glucose microenvironments. Mechanistically, the effects of curcumin on BMSC osteogenic determination and BMSC-mediated angiogenesis were achieved, at least partially, by inhibiting the high glucose-activated NF-κB signaling pathway. Furthermore, we confirmed that curcumin treatment promoted bone regeneration and accelerated angiogenesis in a DM model. To our knowledge, this is the first to confirm that curcumin prevents diabetes-induced bone loss by promoting BMSC-mediated osteogenesis and angiogenesis coupling.

BMSCs are a cell type which have self-renewal and multidirectional differentiation potential. It is well known that osteogenesis ability of BMSCs plays a crucial role in bone repair and regeneration. However, increasing evidence has shown that the decline in the osteogenic function of BMSCs is a vital mechanism for diabetic osteoporosis. BMSCs derived from diabetic patients show a decreased osteogenic differentiation ability [49]. In a high glucose microenvironment, advanced glycation end products (AGEs) induce Wnt/LRP5/β-catenin to inhibit the BMSCs osteogenic differentiation [50]. These studies suggest that hyperglycemia can lead to a change in BMSCs differentiation function, resulting in a decrease in the self-repair and regeneration ability of the bone tissue and related pathological changes in diabetic osteoporosis. Recently, an increasing number of reports have shown that curcumin possesses favorable properties on diabetic bone metabolism [32–34]. Li and Zhang founded that curcumin pretreatment could promote osteogenesis of BMSCs in high glucose and enhanced bone formation in diabetic rats by regulating the Keap1/Nrf2/HO-1 signaling pathway [3]. Another study showed that curcumin enhanced osteogenesis-related gene expressions and suppressed apoptosis in osteoblasts under high glucose microenvironment [35, 36]. In this study, our results showed that curcumin treatment rescued high glucose-inhibited osteogenic differentiation ability of BMSCs *in vitro*. Furthermore, our *in vivo* results also revealed that curcumin prevented bone loss in diabetic mice.

The osteogenesis and angiogenesis coupling is crucial in the process of bone regeneration. There is increasing evidence that BMSCs promote vessel formation in the skeletal system

based on the coupling between osteogenesis and angiogenesis. BMSCs not only induce differentiation into endothelial cells to form vascular-like tissue but also produce multiple proangiogenic growth factors to promote angiogenesis [51, 52]. Moreover, the proangiogenic ability of BMSCs is regulated by many factors. Platelet-derived growth factor-B (PDGF-B) gene overexpression in BMSCs can enhance angiogenesis and promote the repair of bone defects [53]. BMSCs derived from OVX rats showed a decreased angiogenesis ability [11]. Catalpol, a natural iridoid glycoside, accelerates bone regeneration through improving the angiogenesis of BMSCs [13]. However, the influence of curcumin on the ability of BMSCs to regulate angiogenesis has been rarely reported. In this study, we verified that curcumin could rescue the high glucose-impaired angiogenic ability of BMSCs by elevating the expression and secretion of the proangiogenic factor VEGF. Besides, we proved that curcumin treatment promoted vessel formation in the DM model.

Recently, type H vessels were discovered in mouse and human bone tissues that is characterized by the high expression of CD31 and endomucin (CD31^{hi}Emcn^{hi}). Type H vessels secrete factors such as HIF-1α, VEGF, and Notch that promote vessel assembly and bone formation [16, 17]. Given the important role of type H vessels in coupling osteogenesis and angiogenesis, the effect of curcumin on type H vessels in DM mice was investigated. Our results showed a decreased number of type H vessels in DM mice, but curcumin administration increased the quantity of vessels.

Activation of the NF-κB pathway is involved in diabetes and osteoporosis [38–40]. Inhibiting overactivated NF-κB pathway promotes the differentiation and mineralization of MC3T3 cells [54]. NF-κB inhibitor treatment rescues high glucose-dependent inflammatory cytokine expression and PDLSCs osteogenic differentiation [55, 56]. In this study, we found that the activated NF-κB signaling pathway was inhibited by curcumin treatment in BMSCs. Moreover, Bay117082, an NF-κB inhibitor, was used to investigate the role of NF-κB in high glucose-induced BMSCs dysfunction. Our results showed that Bay117082 treatment reversed the glucose-inhibited osteoblastic differentiation and angiogenesis of BMSCs *in vitro*. Taken together, the above results indicated that curcumin rescued the high glucose-impaired osteogenesis and angiogenesis coupling of BMSCs via inhibiting the overactivated NF-κB signaling pathway.

5. Conclusions

Our findings reveal the effects of curcumin in promoting the BMSCs-mediated osteogenesis and angiogenesis coupling in high glucose conditions. These impacts are preliminarily considered to be via NF-κB signaling pathway inhibition. Furthermore, curcumin may become a potential drug to prevent and treat diabetic osteoporosis through promoting bone regeneration and vessel formation.

Data Availability

The data used to support the findings of this study are included within the article.

Conflicts of Interest

The authors declare that they have no conflicts of interest.

Acknowledgments

References

[1] E. M. Dalsgaard, M. V. Skriver, A. Sandbaek, and M. Vestergaard, "Socioeconomic position, type 2 diabetes and long-term risk of death," *PLoS One*, vol. 10, no. 5, Article ID e0124829, 2015.

[2] L. Guariguata, "By the numbers: new estimates from the IDF Diabetes Atlas Update for 2012," *Diabetes Research and Clinical Practice*, vol. 98, no. 3, pp. 524-525, 2012.

[3] Y. Li and Z. Z. Zhang, "Sustained curcumin release from PLGA microspheres improves bone formation under diabetic conditions by inhibiting the reactive oxygen species production," *Drug Design, Development and Therapy*, vol. 12, pp. 1453–1466, 2018.

[4] F. R. Cirano, S. P. Pimentel, M. Z. Casati et al., "Effect of curcumin on bone tissue in the diabetic rat: repair of peri-implant and critical-sized defects," *International Journal of Oral and Maxillofacial Surgery*, vol. 47, no. 11, pp. 1495–1503, 2018.

[5] S. S. Safarova, "Alterations of bone metabolism in patients with diabetes mellitus," *The Internet Journal of Endocrinology*, vol. 2019, Article ID 5984681, 5 pages, 2019.

[6] S. L. Ferrari, B. Abrahamsen, N. Napoli et al., "Diagnosis and management of bone fragility in diabetes: an emerging challenge," *Osteoporosis International*, vol. 29, no. 12, pp. 2585–2596, 2018.

[7] L. Si, T. M. Winzenberg, Q. Jiang, M. Chen, and A. J. Palmer, "Projection of osteoporosis-related fractures and costs in China: 2010–2050," *Osteoporosis International*, vol. 26, no. 7, pp. 1929–1937, 2015.

[8] A. P. Kusumbe, S. K. Ramasamy, and R. H. Adams, "Coupling of angiogenesis and osteogenesis by a specific vessel subtype in bone," *Nature*, vol. 507, no. 7492, pp. 323–328, 2014.

[9] S. K. Ramasamy, A. P. Kusumbe, L. Wang, and R. H. Adams, "Endothelial Notch activity promotes angiogenesis and osteogenesis in bone," *Nature*, vol. 507, no. 7492, pp. 376–380, 2014.

[10] Z. Tan, B. Zhou, J. Zheng et al., "Lithium and copper induce the osteogenesis-angiogenesis coupling of bone marrow mesenchymal stem cells via crosstalk between canonical Wnt and HIF-1α signaling pathways," *Stem Cells International*, vol. 2021, Article ID 6662164, 15 pages, 2021.

[11] H. Jing, L. Liao, X. Su et al., "Declining histone acetyltransferase GCN5 represses BMSC-mediated angiogenesis during osteoporosis," *The FASEB Journal*, vol. 31, no. 10, pp. 4422–4433, 2017.

[12] J. Wu, A. Wang, X. Wang et al., "Rapamycin improves bone mass in high-turnover osteoporosis with iron accumulation through positive effects on osteogenesis and angiogenesis," *Bone*, vol. 121, pp. 16–28, 2019.

[13] L. Chen, R. Y. Zhang, J. Xie et al., "STAT3 activation by catalpol promotes osteogenesis-angiogenesis coupling, thus

accelerating osteoporotic bone repair," *Stem Cell Research & Therapy*, vol. 12, no. 1, p. 108, 2021.

[14] H. Jing, L. Liao, Y. An et al., "Suppression of EZH2 prevents the shift of osteoporotic MSC fate to adipocyte and enhances bone formation during osteoporosis," *Molecular Therapy*, vol. 24, no. 2, pp. 217–229, 2016.

[15] L. Liao, X. Su, X. Yang et al., "TNF-alpha inhibits FoxO1 by upregulating miR-705 to aggravate oxidative damage in bone marrow-derived mesenchymal stem cells during osteoporosis," *Stem Cells*, vol. 34, no. 4, pp. 1054–1067, 2016.

[16] W. Liu, M. Qi, A. Konermann, L. Zhang, F. Jin, and Y. Jin, "The p53/miR-17/Smurf1 pathway mediates skeletal deformities in an age-related model via inhibiting the function of mesenchymal stem cells," *Aging*, vol. 7, no. 3, pp. 205–218, 2015.

[17] Y. Li, L. Fan, J. Hu et al., "MiR-26a rescues bone regeneration deficiency of mesenchymal stem cells derived from osteoporotic mice," *Molecular Therapy*, vol. 23, no. 8, pp. 1349–1357, 2015.

[18] P. Tagde, P. Tagde, F. Islam et al., "The multifaceted role of curcumin in advanced nanocurcumin form in the treatment and management of chronic disorders," *Molecules*, vol. 26, no. 23, p. 7109, 2021.

[19] M. M. Rahman, M. R. Islam, S. Shohag et al., "The multifunctional role of herbal products in the management of diabetes and obesity: a comprehensive review," *Molecules*, vol. 27, no. 5, p. 1713, 2022.

[20] F. Islam, S. Mitra, M. H. Nafady et al., "Neuropharmacological and antidiabetic potential of *Lannea coromandelica* (Houtt.) Merr. leaves extract: an experimental analysis," *Evidence Based Complement Alternative Medicine*, vol. 2022, Article ID 6144733, 10 pages, 2022.

[21] S. Mitra, J. Anjum, M. Muni et al., "Exploring the journey of emodin as a potential neuroprotective agent: novel therapeutic insights with molecular mechanism of action," *Biomedicine & Pharmacotherapy*, vol. 149, Article ID 112877, 2022.

[22] S. Mitra, M. S. Lami, T. M. Uddin et al., "Prospective multifunctional roles and pharmacological potential of dietary flavonoid narirutin," *Biomedicine & Pharmacotherapy*, vol. 150, Article ID 112932, 2022.

[23] D. Allegrini, R. Raimondi, A. Borgia et al., "Curcumin in retinal diseases: a comprehensive review from bench to bedside," *International Journal of Molecular Sciences*, vol. 23, no. 7, p. 3557, 2022.

[24] S. Fuloria, J. Mehta, A. Chandel et al., "A comprehensive review on the therapeutic potential of Curcuma longa Linn. in relation to its major active constituent curcumin," *Frontiers in Pharmacology*, vol. 13, Article ID 820806, 2022.

[25] W. Chen, H. Shi, P. Deng et al., "Quality of evidence supporting the role of curcuma longa extract/curcumin for the treatment of osteoarthritis: an overview of systematic reviews," *Evidence-Based Complementary and Alternative Medicine*, vol. 2022, Article ID 6159874, 14 pages, 2022.

[26] C. Dai, J. Lin, H. Li et al., "The natural product curcumin as an antibacterial agent: current achievements and problems," *Antioxidants*, vol. 11, no. 3, p. 459, 2022.

[27] M. W. Yang, T. H. Wang, P. P. Yan et al., "Curcumin improves bone microarchitecture and enhances mineral density in APP/PS1 transgenic mice," *Phytomedicine*, vol. 18, no. 2-3, pp. 205–213, 2011.

[28] S. Bose, N. Sarkar, and D. Banerjee, "Effects of PCL, PEG and PLGA polymers on curcumin release from calcium phosphate matrix for in vitro and in vivo bone regeneration," *Materials Today Chemistry*, vol. 8, pp. 110–120, 2018.

[29] S. N. A. Bukhari, F. Hussain, H. E. Thu, and Z. Hussain, "Synergistic effects of combined therapy of curcumin and fructus ligustri lucidi for treatment of osteoporosis: cellular and molecular evidence of enhanced bone formation," *Journal of Integrative Medicine*, vol. 17, no. 1, pp. 38–45, 2019.

[30] Q. Jiang, Y. Lei, D. C. Krishnadath, B. Y. Zhu, and X. Zhou, "Curcumin regulates EZH2/Wnt/β-catenin pathway in the mandible and femur of ovariectomized osteoporosis rats," *The Kaohsiung Journal of Medical Sciences*, vol. 37, no. 6, pp. 513–519, 2021.

[31] F. Khanizadeh, A. Rahmani, K. Asadollahi, and M. R. H. Ahmadi, "Combination therapy of curcumin and alendronate modulates bone turnover markers and enhances bone mineral density in postmenopausal women with osteoporosis," *Archives of Endocrinology and Metabolism*, vol. 62, no. 4, pp. 438–445, 2018.

[32] A. Riva, S. Togni, L. Giacomelli et al., "Effects of a curcumin-based supplementation in asymptomatic subjects with low bone density: a preliminary 24-week supplement study," *European Review for Medical and Pharmacological Sciences*, vol. 21, no. 7, pp. 1684–1689, 2017.

[33] Y. Liang, B. Zhu, S. Li et al., "Curcumin protects bone biomechanical properties and microarchitecture in type 2 diabetic rats with osteoporosis via the TGFβ/Smad2/3 pathway," *Experimental and Therapeutic Medicine*, vol. 20, no. 3, pp. 2200–2208, 2020.

[34] J. Deng, L. M. Golub, H. M. Lee et al., "A novel modified-curcumin promotes resolvin-like activity and reduces bone loss in diabetes-induced experimental periodontitis," *Journal of Inflammation Research*, vol. 14, pp. 5337–5347, 2021.

[35] X. Li, Y. Chen, Y. Mao et al., "Curcumin protects osteoblasts from oxidative stress-induced dysfunction via GSK3β-Nrf2 signaling pathway," *Frontiers in Bioengineering and Biotechnology*, vol. 8, p. 625, 2020.

[36] P. Dai, Y. Mao, X. Sun et al., "Attenuation of oxidative stress-induced osteoblast apoptosis by curcumin is associated with preservation of mitochondrial functions and increased Akt-GSK3β signaling," *Cellular Physiology and Biochemistry*, vol. 41, no. 2, pp. 661–677, 2017.

[37] S. Chen, H. Liang, Y. Ji et al., "Curcumin modulates the crosstalk between macrophages and bone mesenchymal stem cells to ameliorate osteogenesis," *Frontiers in Cell and Developmental Biology*, vol. 9, Article ID 634650, 2021.

[38] J. He, X. Yang, F. Liu et al., "The impact of curcumin on bone osteogenic promotion of MC3T3 cells under high glucose conditions and enhanced bone formation in diabetic mice," *Coatings*, vol. 10, no. 3, p. 258, 2020.

[39] C. L. Li, X. H. Liu, Y. Qiao et al., "Allicin alleviates inflammation of diabetic macroangiopathy via the Nrf2 and NF-kB pathway," *European Journal of Pharmacology*, vol. 876, Article ID 173052, 2020.

[40] M. Davari, R. Hashemi, P. Mirmiran et al., "Effects of cinnamon supplementation on expression of systemic inflammation factors, NF-kB and Sirtuin-1 (SIRT1) in type 2 diabetes: a randomized, double blind, and controlled clinical trial," *Nutrition Journal*, vol. 19, p. 1, 2020.

[41] Y. Liu, W. Liu, Z. Yu et al., "A novel BRD4 inhibitor suppresses osteoclastogenesis and ovariectomized osteoporosis by blocking RANKL-mediated MAPK and NF-κB pathways," *Cell Death & Disease*, vol. 12, no. 7, p. 654, 2021.

[42] L. Marinucci, S. Balloni, K. Fettucciari, M. Bodo, V. N. Talesa, and C. Antognelli, "Nicotine induces apoptosis in human

osteoblasts via a novel mechanism driven by H2O2 and entailing Glyoxalase 1-dependent MG-H1 accumulation leading to TG2-mediatedNF-kB desensitization: implication for smokers-related osteoporosis," *Free Radical Biology and Medicine*, vol. 117, pp. 6–17, 2018.

[43] J. Han and W. Wang, "Effects of tanshinol on markers of bone turnover in ovariectomized rats and osteoblast cultures," *PLoS One*, vol. 12, no. 7, Article ID e0181175, 2017.

[44] F. Wang, W. Wang, L. Kong et al., "Accelerated bone regeneration by adrenomedullin 2 through improving the coupling of osteogenesis and angiogenesis via beta-catenin signaling," *Frontiers in Cell and Developmental Biology*, vol. 9, Article ID 649277, 2021.

[45] H. Ma, X. Wang, W. Zhang et al., "Melatonin suppresses ferroptosis induced by high glucose via activation of the Nrf2/HO-1 signaling pathway in type 2 diabetic osteoporosis," *Oxidative Medicine and Cellular Longevity*, vol. 2020, Article ID 9067610, 18 pages, 2020.

[46] Y. Cao, X. Han, Z. Wang et al., "TLR4 knockout ameliorates streptozotocin-induced osteoporosis in a mouse model of diabetes," *Biochemical and Biophysical Research Communications*, vol. 546, pp. 185–191, 2021.

[47] Y. Sun, Y. Zhu, X. Liu, Y. Chai, and J. Xu, "Morroniside attenuates high glucose-induced BMSC dysfunction by regulating the Glo1/AGE/RAGE axis," *Cell Proliferation*, vol. 53, no. 8, Article ID e12866, 2020.

[48] S. S. Qi, M. L. Shao, Z. Sun et al., "Chondroitin sulfate alleviates diabetic osteoporosis and repairs bone microstructure via anti-oxidation, anti-inflammation, and regulating bone metabolism," *Frontiers in Endocrinology*, vol. 12, Article ID 759843, 2021.

[49] W. Shi, D. Ling, F. Zhang, X. Fu, D. Lai, and Y. Zhang, "Curcumin promotes osteogenic differentiation of human periodontal ligament stem cells by inducting EGR1 expression," *Archives of Oral Biology*, vol. 121, Article ID 104958, 2021.

[50] B. Zhang, N. Liu, H. Shi et al., "High glucose microenvironments inhibit the proliferation and migration of bone mesenchymal stem cells by activating GSK3β," *Journal of Bone and Mineral Metabolism*, vol. 34, no. 2, pp. 140–150, 2016.

[51] S. Shi, J. Sun, Q. Meng et al., "Sonic hedgehog promotes endothelial differentiation of bone marrow mesenchymal stem cells via VEGF-D," *Journal of Thoracic Disease*, vol. 10, no. 9, pp. 5476–5488, 2018.

[52] K. Hu and B. R. Olsen, "Osteoblast-derived VEGF regulates osteoblast differentiation and bone formation during bone repair," *Journal of Clinical Investigation*, vol. 126, no. 2, pp. 509–526, 2016.

[53] Z. Shen, Z. Chen, Z. Li et al., "Total flavonoids of rhizoma drynariae enhances angiogenic-osteogenic coupling during distraction osteogenesis by promoting type H vessel formation through PDGF-BB/PDGFR-β instead of HIF-1α/VEGF Axis," *Frontiers in Pharmacology*, vol. 11, Article ID 503524, 2020.

[54] M. Yamazaki, H. Fukushima, M. Shin et al., "Tumor necrosis factor α represses bone morphogenetic protein (BMP) signaling by interfering with the DNA binding of smads through the activation of NF-κB," *Journal of Biological Chemistry*, vol. 284, no. 51, pp. 35987–35995, 2009.

[55] N. Wang, Z. Zhou, T. Wu et al., "TNF-α-induced NF-κB activation upregulates microRNA-150-3p and inhibits osteogenesis of mesenchymal stem cells by targeting β-catenin," *Open Biology*, vol. 6, no. 3, Article ID 150258, 2016.

[56] Z. L. Guo, S. L. Gan, C. Y. Cao et al., "Advanced glycosylated end products restrain the osteogenic differentiation of the periodontal ligament stem cell," *Journal of Dental Science*, vol. 14, no. 2, pp. 146–151, 2019.